

Application of the unstructured variational nodal method in the He-Xe cooled micro reactor

Qizheng Sun^a, Xiaojing Liu^a, Tengfei Zhang^{a*}

^aSchool of Nuclear Science and Engineering, Shanghai Jiao Tong Univ., Shanghai, 200240

*Corresponding author: zhangtengfei@sjtu.edu.cn

1. Introduction

With the advancement of nuclear technology and diverse application demands, advanced reactor designs represented by solid micro reactor have emerged as pivotal directions for future nuclear reactor development. The SIMONS reactor design, proposed by Shanghai Jiao Tong University (SJTU), is a compact, high-power-density micro solid reactor endowed with transportability and inherent safety [1]. The advanced reactor designs pose challenges to neutron transport simulation due to their pronounced heterogeneity and neutron leakage. The complicated resonance effects and significant variation of the core energy spectrum with space make conventional cross-section (XS) generation method insufficient. In addition, the (n, xn) reaction attributed to Be⁹ must be considered, as neglecting it will result in substantial deviations [2]. As a result, high-fidelity transport method and precise XS generation method are indispensable for realistically simulating the neutronic properties of these novel nuclear reactor concepts.

The unstructured variational nodal method (UVNM), which employs the variational principle to solve the even-parity neutron transport equation (NTE), stands as one of the high-fidelity methods for heterogeneous problems with complex geometry [3][4][5]. In order to flexibly represent intricate geometries, the UVNM discretizes the problem domain into unstructured meshes and utilizes the coordinate transformation technique to relate the standard node to the arbitrary node. Concerning angular variables, the discrete-ordinate (S_N) treatment is employed to decouple the original NTE into a series of angular discretized equations. Numerical results demonstrate that the UVNM serves as a flexible toolkit for various applications. Moreover, the UVNM with S_N treatment has been integrated into the models of the VITAS code developed at SJTU [3]. Leveraging its advantages, the VITAS code serves as the transport solver for analyzing the heterogeneous problems of the SIMONS reactor in this study.

To acquire accurate XSs for the transport solver, a precise XS generation process is established based on OpenMC [6]. The out-scatter transport correction is employed to handle the anisotropic scattering [7]. Additionally, the (n, xn) XSs are utilized to generate equivalent transport and scattering XSs, ensuring the consistency of the neutron transport equation (NTE) formulation. Furthermore, the XSs with the same composition in different regions are treated differently due to regionally distinct self-shielding effects and spectrum variation.

Based on the proposed XS generation process, this work conducts simulations of the SIMONS He-Xe cooled microreactor utilizing the VITAS code. The schemes for energy group division for XS generation are assessed. Furthermore, the transport solutions obtained from the UVNM method are analyzed and compared with the continuous-energy solutions obtained from OpenMC.

2. Theoretical Methods

In this section, the theoretical model of UVNM, the out-scatter transport correction, and the treatment of the (n, xn) reaction are described. The fundamental procedure of the UVNM is outlined in this article, and further elucidation regarding the UVNM can be found in Ref. [4,5].

2.1 The UVNM theory

The UVNM transport model starts with the even-parity NTE. Considering isotropic scattering, the steady-state multi-group even-parity NTE can be expressed as

$$-\mathbf{\Omega} \cdot \nabla \Sigma_{t,g}^{-1}(\mathbf{r}) \mathbf{\Omega} \cdot \nabla \psi_g^+(\mathbf{r}, \mathbf{\Omega}) + \Sigma_{t,g}(\mathbf{r}) \psi_g^+(\mathbf{r}, \mathbf{\Omega}) = S_g(\mathbf{r}, \mathbf{\Omega}) \quad (1)$$

The term $S_g(\mathbf{r}, \mathbf{\Omega})$ in Eq. (1) represents the sum of the scattering and fission source

$$S(\mathbf{r}) = \sum_{g'=1}^G \frac{\chi_{g'}}{k_{\text{eff}}} \nu \Sigma_{f,g'}(\mathbf{r}) \phi_{g'}(\mathbf{r}) + \sum_{g'=1}^G \Sigma_{s,g'-g}(\mathbf{r}) \phi_{g'}(\mathbf{r}) \quad (2)$$

where the angular integration is normalized to unity. The subscript g represents the g -th energy group; $\mathbf{r} \in \mathbb{R}^3$ represents the spatial position; $\mathbf{\Omega} \in \mathbb{R}^3$ represents the direction of neutron movement; ψ_g represents the even-parity angular neutron flux for group g ; $\Sigma_{t,g}$ represents the total XS; $\Sigma_{s,g'-g}$ represents the scattering XS from the group g' to g ; $\nu \Sigma_{f,g}$ represents the neutron production by fission contributed by the group g ; χ_g represents the fission spectrum, $\Phi_g(\mathbf{r}, \mathbf{\Omega})$ represents the angular neutron flux of group g , and k_{eff} represents the eigenvalue.

As given in Eq. (3), the UVNM establishes a functional, which implicitly including the even-parity NTE and nodal boundary conditions as part of its stationary conditions. Then the transport problem can be solved using the extremum variational principle.

$$F_v[\psi, \chi] = \int_V dV \left\{ \int_{\Omega} d\Omega \left[\Sigma_t^{-1}(\mathbf{r})(\boldsymbol{\Omega} \cdot \nabla \psi)^2 + \Sigma_t(\mathbf{r})\psi^2 \right] \right. \\ \left. - \Sigma_s(\mathbf{r})\phi^2(\mathbf{r}) - 2\phi(\mathbf{r})S(\mathbf{r}) \right\} \\ + 2 \sum_{\gamma} \int_{\gamma} d\Gamma \int_{\Omega} d\Omega (\mathbf{n}_{\gamma} \cdot \boldsymbol{\Omega}) \chi_{\gamma} \quad (3)$$

where the subscript g is omitted; χ_{γ} represents the odd-parity neutron flux on the surface γ .

Moreover, we define the even-parity flux $\omega_{\gamma}(\mathbf{r}, \boldsymbol{\Omega})$ along the interfaces, which satisfies

$$\omega_{\gamma}(\mathbf{r}, \boldsymbol{\Omega}) = \boldsymbol{\Omega} \cdot \mathbf{n}_{\gamma} \chi_{\gamma}(\mathbf{r}, \boldsymbol{\Omega}) \quad (4)$$

Moreover, the functional is discretized by orthogonal normalized polynomial basis functions in the unstructured node. In addition, the S_N method tackles the problem by independently solving discrete angular directions. In this manner, response matrix equations can be formed by first discretizing the functional in space and angle and then requiring the functional to be stationary with respect to ψ and χ_{γ}

$$\psi_n = \mathbf{H}_n \mathbf{s} - \mathbf{C}_n \omega_n, \quad n = 1, \dots, N \quad (5)$$

$$\mathbf{j}_n^+ = \mathbf{B}_n \mathbf{s} + \mathbf{R}_n \mathbf{j}_n^-, \quad n = 1, \dots, N \quad (6)$$

where the subscript n represents a specific angular direction; \mathbf{s} represents moments of the source term; ω_n represents the moments of $\omega_{\gamma}(\mathbf{r}, \boldsymbol{\Omega})$; \mathbf{j}_n^+ and \mathbf{j}_n^- represent the outgoing and incoming partial current, respectively. All response matrices (RMs) used in Eqs. (5) and (6) are constructed as given in Table I.

Table I RMs of UVNM

$A_n = \sum_{i,j=x,y,z} \Omega_{n,i} \Omega_{n,j} P_{i,j} + \Sigma_t I_V$
$P_{i,j} = \Sigma_t^{-1} \int_V (\nabla_i f)(\nabla_j f^T) dV \quad i, j = x, y, z$
$E_{\gamma}(\mathbf{r}) = \int_{\gamma} \mathbf{f} \mathbf{h}^T d\Gamma$
$\mathbf{H}_n = A_n^{-1} I_V$
$\mathbf{C}_n = A_n^{-1} E$
$\mathbf{B}_n = \frac{1}{2} (\mathbf{G}_n + \mathbf{I})^{-1} \mathbf{C}^T I_V$
$\mathbf{R}_n = (\mathbf{G}_n + \mathbf{I})^{-1} (\mathbf{G}_n - \mathbf{I})$
$\mathbf{G}_{n,\gamma\gamma'} = \frac{1}{2} E_{\gamma}^T A_n^{-1} E_{\gamma'}$

2.2 Transport XSs correction

In order to procure dependable transport solutions using UVNM, the incorporation of anisotropic scattering becomes crucial, particularly for fast or mixed-spectrum reactor challenges. To address this issue, the scattering matrix multi-group XSs with the cosine of the change-in-angle are expanded into Legendre basis functions.

$$\Sigma_{s,g'-g}(\mathbf{r}, \boldsymbol{\Omega} \cdot \boldsymbol{\Omega}') = \sum_{l=0}^L \Sigma_{s,g'-g,l}(\mathbf{r}) P_l(\boldsymbol{\Omega} \cdot \boldsymbol{\Omega}') \quad (7)$$

Where L represents the expansion order of the Legendre functions.

From the view point of memory usage and computational efficiency, the transport correction is desirable for considering anisotropic scattering. In this work, the transport correction of the out-scatter approximation is employed because it tends to show a higher accuracy than the in-scatter approximation [7]. Therefore, the transport corrected XS can be expressed as

$$\Sigma_{tr,g} = \Sigma_{t,g} - \sum_{g'} \Sigma_{s,1,g-g'} \quad (8)$$

$$\Sigma_{s,g-g'} = \Sigma_{s,0,g-g'} - \delta_{gg'} \sum_{g''} \Sigma_{s,1,g-g''} \quad (9)$$

where $\delta_{gg'}$ represents the Kronecker delta; $\Sigma_{s,0,g-g'}$ and $\Sigma_{s,1,g-g'}$ represent the P_0 and P_1 scattering components, respectively.

By adopting the correction, the P_1 scattering is approximately taken into account, and thus only the P_0 scattering is explicitly used in the transport calculation.

2.3 (n,xn) reaction treatment

The (n,xn) reaction is a neutron multiplication process. In certain materials within the reactor, such as ^9Be , which serves as the reflector material in SIMONS, the occurrence of a significant (n,xn) reaction can lead to a notable neutron multiplication effect. Neglecting the multiplication effects caused by this reaction will destroy the neutron balance, and consequently, transport solutions based on XSs without consideration of the (n,xn) reaction will yield considerable discrepancies.

To consider the (n,xn) reaction, the even-parity NTE can be rewritten as

$$-\boldsymbol{\Omega} \cdot \nabla \Sigma_{t,g}^{-1}(\mathbf{r}) \boldsymbol{\Omega} \cdot \nabla \psi_g^+(\mathbf{r}, \boldsymbol{\Omega}) + \hat{\Sigma}_{t,g}(\mathbf{r}) \psi_g^+(\mathbf{r}, \boldsymbol{\Omega}) \\ = \sum_{g'=1}^G \Sigma_{n1n}^{g'-g}(\mathbf{r}) \phi_{g'}(\mathbf{r}) + 2 \sum_{g'=1}^G \Sigma_{n2n}^{g'-g}(\mathbf{r}) \phi_{g'}(\mathbf{r}) \\ + 3 \sum_{g'=1}^G \Sigma_{n3n}^{g'-g}(\mathbf{r}) \phi_{g'}(\mathbf{r}) + 4 \sum_{g'=1}^G \Sigma_{n4n}^{g'-g}(\mathbf{r}) \phi_{g'}(\mathbf{r}) \\ + \sum_{g'=1}^G \frac{\chi_g}{k_{\text{eff}}} \nu \Sigma_{f,g'}(\mathbf{r}) \phi_{g'}(\mathbf{r}) \quad (10)$$

with

$$\hat{\Sigma}_{t,g} = \Sigma_{n1n}^{g'-g} + \Sigma_{n2n}^{g'-g} + \Sigma_{n3n}^{g'-g} + \Sigma_{n4n}^{g'-g} \quad (11)$$

where $\hat{\Sigma}_{t,g}$ represents the total XS with (n,xn) reaction; $\Sigma_{n1n}^{g'-g}$ represents $(n,1n)$ XS or scattering XS $\Sigma_{s,g-g'}$; $\Sigma_{n2n}^{g'-g}$, $\Sigma_{n3n}^{g'-g}$, $\Sigma_{n4n}^{g'-g}$ represent $(n,2n)$, $(n,3n)$, and $(n,4n)$ XSs, respectively.

To facilitate the calculation, equivalent absorption and scattering XSs are defined, ensuring that the form of the even-parity NTE remains constant. Thus, the reduced absorption XS is defined as

$$\hat{\Sigma}_{a,g} \equiv \Sigma_{a,g} - \Sigma_{n2n}^{g'-g} - 2 \Sigma_{n3n}^{g'-g} - 3 \Sigma_{n4n}^{g'-g} \quad (12)$$

The production scattering XSs are defined as

$$\hat{\Sigma}_{s,g'-g} \equiv \Sigma_{n1n}^{g'-g} + 2\Sigma_{n2n}^{g'-g} + 3\Sigma_{n3n}^{g'-g} + 4\Sigma_{n4n}^{g'-g} \quad (13)$$

With the utilization of the reduced absorption and production scattering XSs, the neutron balance can be preserved, and Eq.(10) can be rewritten as

$$\begin{aligned} & -\mathbf{\Omega} \cdot \nabla \Sigma_{t,g}^{-1}(\mathbf{r}) \mathbf{\Omega} \cdot \nabla \psi_g^+(\mathbf{r}, \mathbf{\Omega}) + \hat{\Sigma}_{t,g}(\mathbf{r}) \psi_g^+(\mathbf{r}, \mathbf{\Omega}) \\ & = \sum_{g'=1}^G \hat{\Sigma}_{s,g'-g}(\mathbf{r}) \phi_{g'}(\mathbf{r}) + \sum_{g'=1}^G \frac{\chi_g}{k_{\text{eff}}} \nu \Sigma_{f,g'}(\mathbf{r}) \phi_{g'}(\mathbf{r}) \end{aligned} \quad (14)$$

with

$$\hat{\Sigma}_{t,g} = \hat{\Sigma}_{a,g} + \sum_{g'} \hat{\Sigma}_{s,g-g'} \quad (15)$$

3. Numerical results

Based on the transport correction and (n, xn) treatment, the XSs of SIMONS can be generated accurately for the UVNM transport simulation. In this section, we seek to compare the transport solutions of UVNM with the continuous energy Monte-Carlo solutions of OpenMC to verify the proposed method. A two-dimensional whole-core SIMONS model is established and analyzed.

The SIMONS problem consists of five materials: monolith, fuel, He-Xe coolant, cladding, and reflector. The monolith, made of graphite, contains hexagonally arranged holes to accommodate the fuel and He-Xe coolant. Detailed geometrical and material information is given in Table II. More information about SIMONS can be found in Ref [1].

Table II Geometrical and material of the 2D SIMONS problem

Parameter	Value
Fuel diameter (cm)	1.5
He-Xe Coolant diameter (cm)	0.8
He-Xe cladding thickness (cm)	0.05
Fuel to He-Xe Pitch	1.5
Fuel pin numbers	1015
Radius of the monolith (cm)	45
Radial reflector thickness (cm)	20
Fuel material	19.75% UC
Cladding	Mo-TZM
Monolith	Graphite
Reflector	Be
Coolant	He-Xe

In this work, the P_0 scattering XSs, high order (P_1) scattering XSs, and (n, xn) XSs are acquired by the open-source code OpenMC. Subsequently, the out-scatter transport correction and (n, xn) correction, as described in Sections 2.2 & 2.3, are applied,

respectively, to derive the final corrected equivalent XSs.

Moreover, due to regionally distinct self-shielding effects and spectrum variation, XS generation necessitates consideration of both material properties and spatial regions. Specifically, the XSs of graphite monolith and the He-Xe coolant are generated based solely on the material type. Besides, the outermost ring, second outermost ring, and inner fuel pins are treated differently for the XS generation. Moreover, the 3.5 cm thick reflector located outside of the monolith is partitioned and treated as a distinct entity, as illustrated in Fig. 1. Besides, in order to increase the neutron tally scores for the material with a small volume, the He-Xe coolant and the cladding are homogenized as a unity to generate XSs.

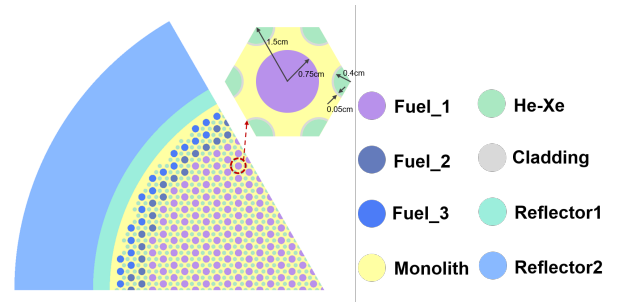


Fig. 1 Diagram of the one-sixth geometrical model for XS generation.

Following the aforementioned scheme, the one-sixth OpenMC model of SIMONS is built. The OpenMC model employs the ENDF VII.I database at 298K, with 2,000,000 particle histories, 400 total cycles, and 150 inactive cycles. The k_{eff} of the OpenMC continuous energy result is 1.22009 ± 0.00006 . Additionally, the normalized neutron spectrum of the whole model is tallied, as depicted in Fig. 2. Fig. 2 exhibits peaks in both the thermal and fast spectrum regions, indicating that the SIMONS reactor holds a mixed spectrum property.

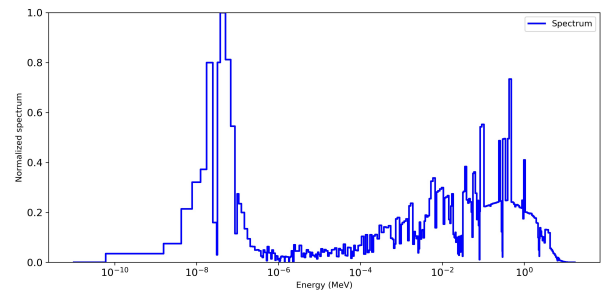


Fig. 2 The whole model normalized spectrum of SIMONS reactor.

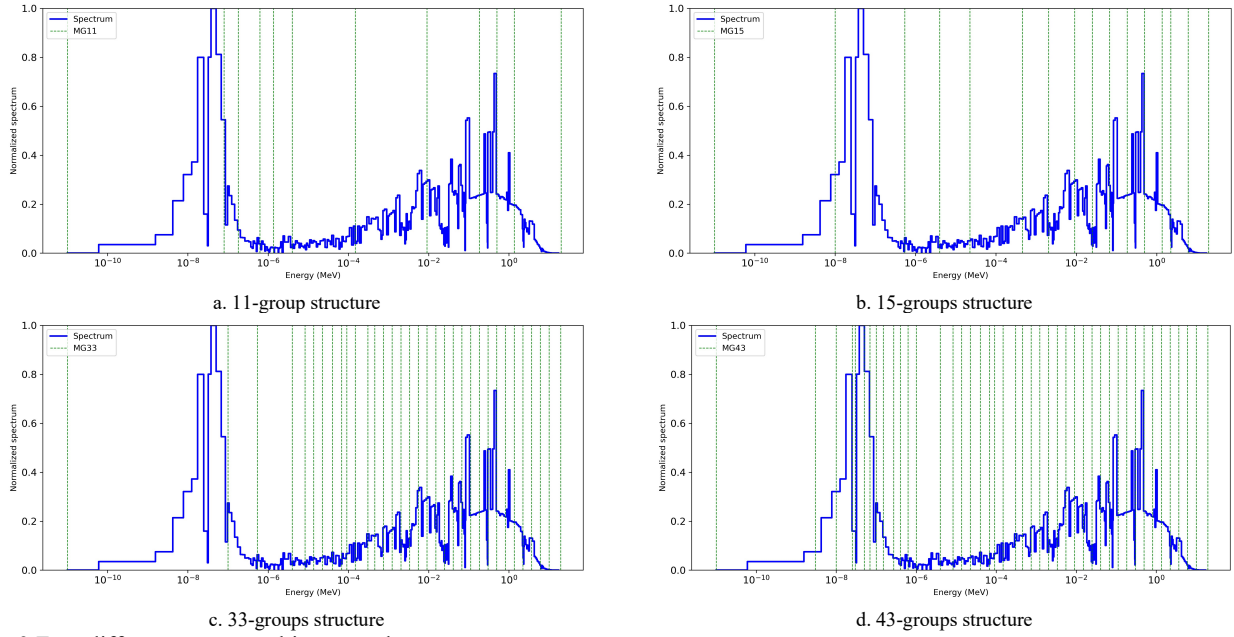


Fig. 3 Four different energy multi-group edges.

This work evaluates four different multi-group structures for the SIMONS problem, including the 11-group structure [8], the ECCO-33 group structure [9], a 15-group structure collapsed from ECCO-33, and a 43-group structure by refining the thermal groups of ECCO-33. The group edges for these four structures are shown in Fig. 3.

According to the multi-group XS generation model, unstructured meshes covering the entire problem domain are generated using the open-source mesh generator Gmsh [10] for UVNM transport simulation, of which one-sixth are illustrated by Fig. 4.

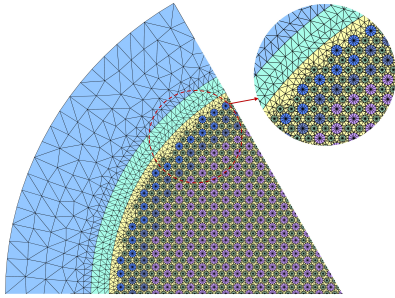


Fig. 4 Unstructured meshes for one-sixth of the whole model for UVNM transport simulation.

After sensitivity analysis, the UVNM transport simulation was performed based on VITAS code using 2nd/1st spatial expansion orders within and along the interfaces of nodes, and 18th/10th Legendre-Chebyshev angular expansion in radial and axial, respectively. The 2-norm tolerances for k_{eff} , flux, and fission source are set as 1.0E-6, 5.0E-5, and 5.0E-5, respectively. All cases are executed with 120 MPI ranks distributed across ten nodes of the SJTU Pi2.0 cluster.

Table III presents the k_{eff} results of VITAS with four different multi-group structures. The table indicates that the k_{eff} results of the VITAS transport simulations converge as the number of multi-groups increases. Notably, when the multi-group number is raised to 33, the k_{eff} result tends to stabilize with an error of 37 pcm compared to the OpenMC reference solution. In addition, the k_{eff} error shows significant improvement from the 11-group structure to the 15-group structure. This enhancement can be attributed to the further refinement of the 15-group structure in the fast spectrum region.

Table III Comparison of k_{eff} results between the VITAS code under different multi-group structures and the OpenMC code.

Code	Number of group	k_{eff}	k_{eff} error (pcm)
OpenMC	-	1.22009 ± 0.00006	-
	11	1.22529	520
VITAS	15	1.22192	183
	33	1.22046	37
	43	1.22054	45

Furthermore, the 33-group structure results of the VITAS transport simulation were analyzed as a representation. Fig. 5 depicts the normalized power distribution obtained from VITAS. The fuel pins at the outer rings in Fig. 5 exhibit a relatively higher power level, attributed to the moderation effect of the reflector. Additionally, the pin power errors between the solutions of VITAS and OpenMC are visualized in Fig. 6, where the maximum error, the minimum error, and the average error of the absolute values are 1.69%, -0.74%, and 0.53%, respectively. The errors of the fuel pins inside the core do not exceed 1% and demonstrate a relatively uniform distribution. On the other hand, the dominant errors are mainly located at the outer rings, with pins

having errors larger than 1.5% highlighted with red edges. Notably, for most of the pins at the outer ring, the power errors are less than 1.5%, indicating a satisfactory agreement between the VITAS transport and the OpenMC continuous energy results.

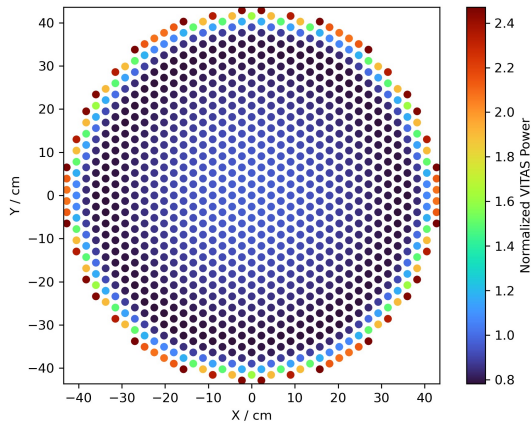


Fig. 5 The normalized power distribution of the VITAS transport simulation.

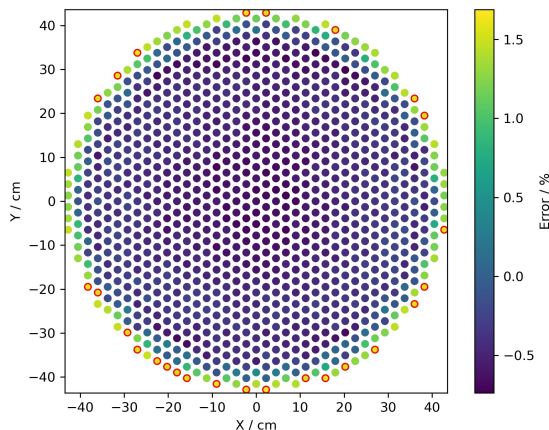


Fig. 6 The relative power error distribution between the VITAS and OpenMC solutions.

4. Conclusions

This work conducts a precise simulation for the 2-D He-Xe cooled microreactor SIMONS, utilizing the UVNM high-fidelity transport method and exact XS generation techniques. The out-scatter transport correction and the (n, xn) correction are implemented, and materials are treated distinctly according to regional considerations during the XS generation. Besides, various multi-group XSs were evaluated in VITAS to obtain high-fidelity transport solutions. The 33-group XSs result obtained by VITAS tends to stabilize, with a k_{eff} error of 37 pcm compared to the OpenMC reference solution. Furthermore, the average pin power error of 0.53% indicates a satisfactory agreement between the VITAS transport and the OpenMC continuous energy results.

Acknowledgements

The authors gratefully acknowledge the support provided by the National Key R&D Program of China under grant number 2020YFB1901900, the National Natural Science Foundation of China 12175138, Shanghai Rising-Star Program, LingChuang Research Project of China National Nuclear Corporation

REFERENCES

- [1] X. Li, X. Liu, X. Chai, T. Zhang, Preliminary Multi-physics Coupled Simulation of Small Helium-Xenon Cooled Mobile Nuclear Reactor, in: Springer Proc. Phys., 2023: pp. 690–702. https://doi.org/10.1007/978-981-99-1023-6_59.
- [2] Fischer J. George, Cross Section for the $(n,2n)$ Reaction in Be9, Phys. Rev. (1957).
- [3] T. Zhang, W. Xiao, H. Yin, Q. Sun, X. Liu, VITAS: A multi-purpose simulation code for the solution of neutron transport problems based on variational nodal methods, Ann. Nucl. Energy. 178 (2022) 109335. <https://doi.org/10.1016/J.ANUCENE.2022.109335>.
- [4] Q. Sun, W. Xiao, X. Li, H. Yin, T. Zhang, X. Liu, A variational nodal formulation for multi-dimensional unstructured neutron diffusion problems, Nucl. Eng. Technol. (2023). <https://doi.org/10.1016/j.net.2023.02.021>.
- [5] Q. Sun, T. Zhang, X. Liu, X. Chai, J. Xiong, A DISCRETE-ORDINATES VARIATIONAL NOCAL METHOD for SOLVING MULTIDIMENSIONAL NEUTRON TRANSPORT EQUATION with UNSTRUCTURED MESH, in: Int. Conf. Nucl. Eng. Proceedings, ICONE, 2022. <https://doi.org/10.1115/ICONE29-91525>.
- [6] P.K. Romano, N.E. Horelik, B.R. Herman, A.G. Nelson, B. Forget, K. Smith, OpenMC: A state-of-the-art Monte Carlo code for research and development, Ann. Nucl. Energy. 82 (2015). <https://doi.org/10.1016/j.anucene.2014.07.048>.
- [7] A. Yamamoto, Y. Kitamura, Y. Yamane, Simplified treatments of anisotropic scattering in LWR core calculations, J. Nucl. Sci. Technol. 45 (2008). <https://doi.org/10.3327/jnst.45.217>.
- [8] N. Stauff, K. MO, Y. Cao, J. Thomas, Y. Miao, L. Zou, D. Nunex, E. Shemon, B. Feng, K. Ni, Detailed analyses of a TRISO-fueled microreactor Modeling of a Micro-Reactor System using NEAMS tools Nuclear Science and Engineering Division, (2021). <https://doi.org/10.2172/1826285>.
- [9] E. Sartori, OECD/NEA Data Bank: Standard Energy Group Structures of Cross Section Libraries for Reactor Shielding, Reactor Cell and Fusion Neutronics Applications: VITAMIN-J, ECCO-33, ECCO-2000 and XMAS JEF/DOC-315 Revision 3 - DRAFT, 1990.
- [10] C. Geuzaine, J.F. Remacle, Gmsh: A 3-D finite element mesh generator with built-in pre- and post-processing facilities, Int. J. Numer. Methods Eng. 79 (2009) 1309–1331. <https://doi.org/10.1002/nme.2579>.